ROYAL SOCIETY
OF CHEMISTRY

COMMUNICATION

CrossMark
← click for updates

Large range electrically-induced reflection notch tuning in polymer stabilized cholesteric liquid crystals

Kyung Min Lee,[ab] Vincent P. Tondiglia,[ac] Taewoo Lee,[d] Ivan I. Smalyukh[d] and Timothy J. White*[a]

This communication reports large magnitude (exceeding 1500 nm) and reversible reflection notch tuning in polymer stabilized cholesteric liquid crystals (PSCLCs) formulated with negative dielectric anisotropy $(-\Delta\varepsilon)$ hosts upon application of a direct current (DC) field. Selective and repeatable tuning ranges of 100 nm to 400 nm are demonstrated. The reflection changes are dictated by a nonlinear distortion of the pitch across the cell thickness, which is associated with electromechanical displacement of the polymer stabilizing network. The electro-optical control of the selective reflection in $-\Delta\varepsilon$ PSCLCs may have potential use in optics, displays, and other commercial products.

Introduction

Cholesteric liquid crystals (CLCs) are self-assembled, one dimensional photonic bandgap materials. The chiral nature of the materials or mixtures dictate either a right handed (RH) or left handed (LH) rotation of the liquid crystal director along a helical axis.[1,2] Accordingly, a single CLC optical element only reflects 50% of unpolarized light. The reflection bandgap of CLCs is centered at the wavelength: $\lambda_0 = n_{avg} \times p_0$, where n_{avg} is the average refractive index of the LC and p_0 is the cholesteric pitch length. The static bandwidth of CLCs in the visible wavelength is a few tens of nanometers, typically 50–100 nm and a product of LC birefringence and cholesteric pitch length, $\Delta\lambda \approx \Delta n \times p_0$. It is noted that $\Delta n = (n_e - n_o)$, where n_e and n_o are the extraordinary and the ordinary refractive index, respectively.

Electrically-induced dynamic optical responses have been examined in CLCs or polymer stabilized CLCs (PSCLCs) including reflection notch switching,[3–16] broadening,[17–24] and tuning.[25–32] Most commonly, the dynamic changes in the reflection of CLCs or PSCLCs are observed by inducing tilt in the pitch in samples

[a] *Air Force Research Laboratory, Materials and Manufacturing Directorate, Wright-Patterson Air Force Base, Ohio, USA. E-mail: Timothy.White.24@us.af.mil; Fax: +019372551128; Tel: +019372559551*
[b] *Azimuth Corporation, Dayton, Ohio, USA*
[c] *Leidos, Beavercreek, Ohio, USA*
[d] *Department of Physics, University of Colorado, Boulder, Colorado, USA*

formulated with nematic liquid crystals with positive dielectric anisotropy $(+\Delta\varepsilon)$.[3–5] The proposed mechanism is electrically induced refractive index changes of $+\Delta\varepsilon$ liquid crystal as the pitch tilts.[31,32] Another approach is to employ interdigitated electrodes to induce local changes in the pitch of CLCs. However, this approach can be hindered by the large electric fields that are required as well as the non-uniform coloration is observed due to complex interdigitated electrode geometry.[28–30] Very recently, large-range color tuning has been observed in CLCs prepared from so-called twist-bend nematic formulations.[33]

Our recent examinations have detailed reflection notch broadening[17–19] in PSCLCs formulated with negative dielectric anisotropy $(-\Delta\varepsilon)$ nematic liquid crystals. As much as a seven-fold increase in bandwidth[17–19] has been observed when these materials are subject to moderate DC fields (0–6 V μm^{-1}). The bandwidth broadening is symmetric about the center of the reflection notch and returns to original bandwidth upon removal of the electric fields. Bandwidth broadening is only observed in samples which are composed of $-\Delta\varepsilon$ nematic liquid crystal hosts, with polymer stabilization, and in the presence of a DC field.

Simplified examinations of nematic and twisted nematic orientations prepared from related compositions indicate that the polymer stabilizing network is delocalized upon application of a DC bias and that the movement of the network is sensitive to the polarity of the DC bias[18,20] Subsequent examination has confirmed that the polymer stabilizing network formed in the presence of the low-molar mass CLC mixture retains a "structural chirality" that can overrule the natural "chemical chirality" of the low-molar mass CLC mixture.[19] Commercial liquid crystal mixtures contain ionic impurities (10^9–10^{14} ions per cm^3), which might come from synthetic and/or purification steps (catalysts, salts, moisture, and dust), alignment layers,[34] and/or degradation of the LC molecules.[35–38] Application of a DC bias to PSCLCs exhibiting so-called "structural chirality" will act upon the native ionic impurities in the mixture[39–42] that are trapped on or within the polymer stabilizing network.[18] Due to the polarity of the DC bias, the polymer stabilizing network is subject to a directional electromechanical force that distorts the structural chirality.

This distortion then affects the anchoring of the low-molar mass CLC mixture resulting in broadening of the reflection band due to nonuniformity in the pitch length of the CLC across the cell gap.[18] Employing $-\Delta\varepsilon$ nematic liquid crystal hosts is critical to enabling this mechanism as the low-molar mass liquid crystalline molecules do not reorient at low to moderate field strengths.

In a related report, electrically-induced tuning in PSCLCs was also observed in samples prepared from $-\Delta\varepsilon$ nematic liquid crystals but composed with comparatively higher polymer concentrations (up to 20 wt%). Due to the large polymer concentration, the optical properties of the PSCLCs both before and during reflection wavelength tuning exhibit substantial haze and poor transmission. Here, we report large magnitude and high optical quality reflection wavelength tuning in PSCLCs formulated with $-\Delta\varepsilon$ nematic liquid crystal hosts. Further, we confirm that the tuning is a result of nonuniform pitch displacement across the cell gap. The large tuning range, high out of band transmission, and electrically controllable position of the spectral reflection of the PSCLCs examined here are potentially useful in many application areas such as displays, smart windows, and optical systems.

Materials and methods

Preparation of $-\Delta\varepsilon$ PSCLCs

The PSCLC samples were prepared by using cells with 15 μm thickness. The cells were coated with alignment layers from a polyimide (PI2555, HD Microsystem) which was rubbed to induce planar alignment. The cells were filled with a mixture containing 1 wt% of photoinitiator (Irgacure 369), chiral dopants (either R1011 and R811 or S1011 and S811, procured from Merck), 5 wt% of a chiral liquid crystal monomer (SLO4151, right handed, procured from Alpha Micron Inc.), and a $-\Delta\varepsilon$ nematic liquid crystal ZLI-2079 ($\Delta\varepsilon = -6.1$ and $\Delta n = 0.15$, procured from Merck). The mixture was photopolymerized by exposing the cells to 80–100 mW cm^{-2} of 350–500 nm UV light (Exfo) for 3 min. To ensure near-uniform through-thickness photopolymerization, the cell was mechanically rotated during UV irradiation. For imaging the depth profile of the pitch of PSCLC samples using three dimensional three-photon excitation fluorescence polarizing microscopy (3PEF-PM) technique, the standard PSCLC formulation was adapted such that it was composed of 6 wt% total monomer concentration (4 wt% SLO4151 and 2 wt% RM23).

Experimental setup and measurements

Transmission and reflection spectra were collected using either right handed circularly polarized or unpolarized light incident on the PSCLC cell. Ion densities of the liquid crystal host (ZLI-2079) and mixtures were quantified by filling 4 μm thickness homeotropic alignment cells. Phase/defect and reflection colour changes were monitored with polarized optical microscopy (POM, Nikon) (transmission and reflection mode) in the presence of DC fields.

The 3PEF-PM imaging was done at room temperature using a multimodal nonlinear optical polarizing microscopy setup integrated with an inverted microscope (IX-81 Olympus) and a galvano-mirror scanning unit (FV300, Olympus).[43,44] The linearly polarized excitation light at 870 nm from a tunable Ti:Sapphire laser (Chameleon Ultra II, Coherent) was focused into the sample using an oil-immersion objective lens (UPlanSApo, 100×, numerical aperture NA = 1.4, from Olympus). The fluorescence signals from the sample were collected by the same objective lens and detected in the range within 390–450 nm in epi-detection mode using a photomultiplier tube and spectral filters while applying different DC fields to the sample. To obtain 3D scans and for cross-sectional imaging across the sample thickness, the motion of the objective lens along the microscope's optical axis was controlled by a stepper motor. The fluorescence signal originating from the polymer network in the PSCLC samples reveals the position of "cholesteric layers" corresponding to half-pitches along the depth, which were typically examined in cross-sectional images. Stacks of 2D images represented three-dimensional molecular orientation field, in which the LC monomer RM23 generated fluorescence signal due to the three-photon-absorption-based excitation. The 3PEF-PM fluorescence signals arising due to the nonlinear optical processes exhibit a strong well-defined dependence of the fluorescence intensity on the orientation of the linear polarization of the excitation beam relative to the spatially varying director. When the excitation light in a probed voxel (3D pixel) is polarized parallel to local molecular orientation direction (director), 3PEF-PM intensity is at maximum (i.e. bright lines). When the polarization of excitation light and director are mutually orthogonal, it is at minimum, i.e. corresponding to the dark lines in the depth-resolved images. The axial spatial resolution to distinguish the individual half-pitches is about 0.4 μm in the orientation sensitive 3PEF-PM setup with the three-photon-absorption-based excitation in the near-IR spectral range, although it can be worsened by factors such as weak fluorescence emission, depolarization, defocusing, and light scattering.[44]

Results and discussion

Large range, electrically-induced tuning of the reflection notch of the PSCLCs prepared and examined here is illustrated in Fig. 1. The as formulated initial notch position (λ_0) of the PSCLC is approximately 700 nm. Application of 160 V (10.7 V μm^{-1}) shifts the reflection notch to nearly 2500 nm. Upon removal of the applied DC field the reflection notch returns to its original notch position. The tuning range of the PSCLC as a function of applied DC field is summarized in Fig. 1(b). The transmission spectra evident in Fig. 1(a) confirm that the PSCLC exhibits good optical quality throughout the entire tuning range. This is in contrast to our recent report[25] where we documented 300–400 nm at 9 V μm^{-1} in a PSCLC with a rather large polymer concentration of 20 wt% with low optical quality in transmission.[25]

The helical structure of a CLC reflects either right handed (RH) or left handed (LH) circularly polarized light (CPL). Fig. 2(a–c) plots the transmission and reflection spectra of RH PSCLCs when probed with RH circularly polarized light before and during the application
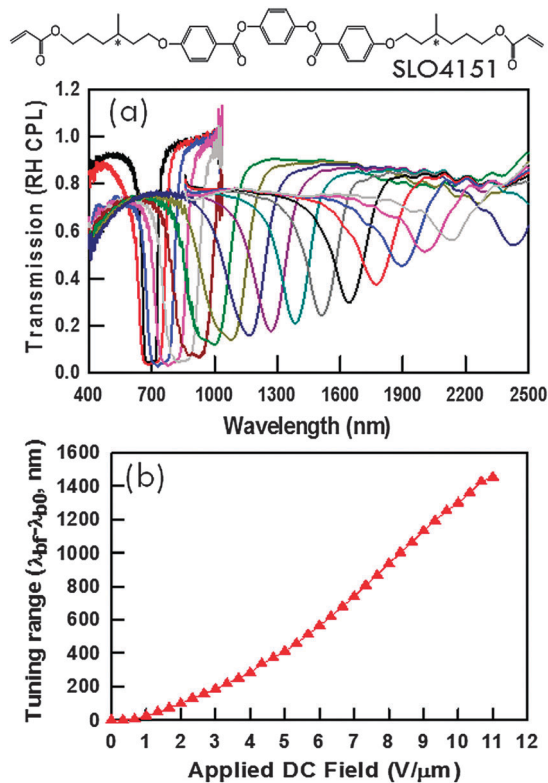
Fig. 1 (a) Transmission spectra of a PSCLC prepared with 5 wt% chiral liquid crystal monomer (SLO4151, inset chemical structure) with increasing DC voltages from 0 V to 160 V. Scanning rate was 1 V sec^{-1}. (b) The relative tuning range of the center of the reflection wavelength (▲) is plotted as a function of applied DC field.
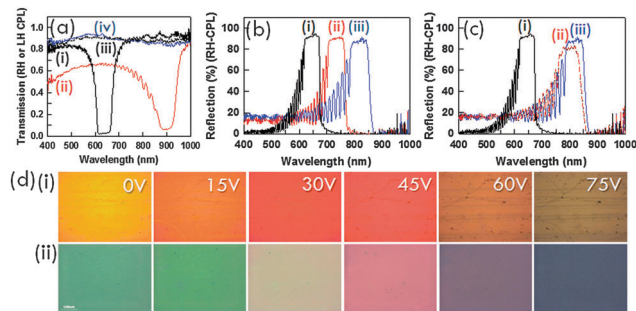

Fig. 2 (a) Transmission spectra of a RH PSCLC when probed with RH circularly polarized light (i and ii) and LH circularly polarized light (iii and iv) at 0 V and 70 V. (b) Reflection spectra at 0 V (i, black), 40 V (ii, red), and 60 V (iii, blue). (c) Reflection spectra of the PSCLC at 0 V (i, black), 60 V (ii, blue), and −60 V (iii, dotted red). (d) POM images in (i) reflection and (ii) transmission with increasing DC voltages from 0 V to 75 V.

of applied DC bias. In Fig. 2(a), the reflection notch apparent at 630 nm is shifted to 900 nm at 70 V DC. When the PSCLC is probed with LH CPL, the sample is optically transparent at both 0 V and 70 V. Fig. 2(b) presents reflection spectra of the same sample when probed with RH CPL at 0, 40, and 60 V. Application of the DC bias shifts the reflection bandgap from 630 nm to as much as 830 nm (60 V). Importantly, the reflectivity of the sample is maintained over this range. Fig. 2(c) plots reflection spectra of the PSCLC sample at 0 V and ±60 V. The reflection spectra at +60 V and −60 V DC bias are nearly identical which confirms that the cell is close to homogenous. Finally, the color as well as the phase and defect structure of the PSCLCs was examined with polarized optical microscopy in both transmission and reflection (Fig. 2(d)). As evident in the spectra in Fig. 1 and 2, reversible and repeatable color changes with high optical quality are observed by the application and removal of the DC voltage. The tuning was repeated more than 50 times with appreciable fatigue. Color changes from orange-yellow to orange to red and ultimately to the infrared region are observed as the DC field increases from 0 V to 75 V.

The ability to modulate the position of the selective reflection of the PSCLCs is shown in Fig. 3(a). Here, the electric field is immediately applied (50 V DC to shift 100 nm) and then held for 30 min. After the field is removed, the reflection wavelength returns to the original position. Thereafter, the same procedure

is repeated for 200 nm (60 V), 300 nm (69 V), and 400 nm (87 V) displacements of the reflection notch. Over the course of 30 min, the reflection notch continues to creep and the magnitude of the creep is dependent on the strength of the applied field. The relaxation times evident in Fig. 3(a) are on the order of minutes. However, this is large part due to the length of time in which the polymer stabilizing network was distorted in the presence of the DC field. To confirm this, Fig. 3(b) plots the position of the center of the reflection notch of a PSCLC upon direct application of 69 V DC (300 nm tuning). Here, the field was applied for 1 min. The relaxation time of the PSCLC is considerably reduced by shortening the duration of the holding voltage. The sensitivity of the PSCLC to the duration of the applied field is related to the mechanics of distorting the crosslinked polymer stabilizing network.
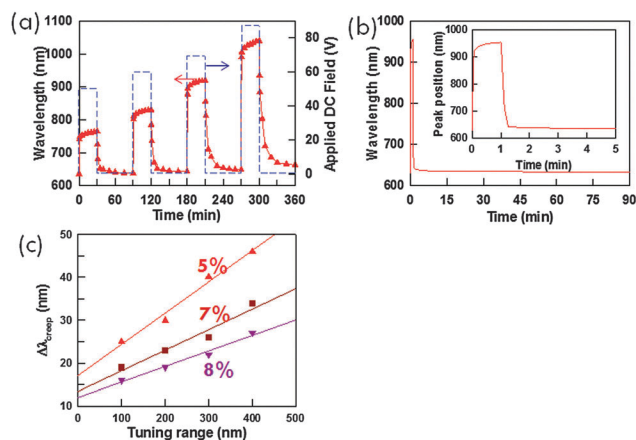

Fig. 3 (a) Variation in reflection wavelength (▲) of a PSCLC with 5 wt% polymer concentration in an experiment in which DC voltages of 50 V, 60 V, 69 V, and 87 V (the strength of the DC voltage is plotted as – –). The voltages were directly applied to the cells and continuously for 30 min. (b) The position of the center of the reflection notch for a PSCLC to direct application of 69 V DC (1 min duration) and relaxation after removal of the applied DC voltage. (c) Relative shift in the position of the reflection wavelength in PSCLCs prepared with 5, 7, and 8 wt% polymer (crosslinker) concentrations to 30 min of continuously applied DC field. $\Delta\lambda_{creep}$ is calculated by taking the reflection wavelength at 30 minutes and subtracting the reflection wavelength at 1 minute.

The relationship between the viscoelasticity of the polymer network and the electro-optic response is further elucidated in Fig. 3(c). Here, PSCLCs were prepared with increasing polymer concentrations (and crosslink densities). The change in wavelength over the course of 30 minutes of continuously applied field is summarized as $\Delta\lambda_{creep}$, which is the difference in the reflection notch position at 1 minute and 30 minutes of continuously applied DC field. Two trends are evident in Fig. 3(c). First, increasing the polymer concentration (crosslink density) reduces the amount of creep in the wavelength shift to continuously applied field. Second, as also evident in Fig. 3(a), the magnitude of creep in wavelength to continuously applied field for 30 minutes is sensitive to the relative displacement of the notch position.

Our initial examination of electrically-induced bandwidth broadening[17] of related formulations mentioned several potential mechanisms for the induced changes to the reflection bandgap. Recently, we have documented[18,20] a series of electro-optic experiments that strongly indicate that the mechanism is ionic in nature and attributable to displacement of the polymer network within the PSCLC. For example, the displacement of the polymer network is visually observed in control experiments employing alignment cells with patterned electrodes wherein the polymer network aggregates on the negatively charged electrodes.[20] Spatial pitch variation is induced by the displacement of polymer network which induces linear-pitch variation for symmetrical dynamic broadening and non-linear pitch variation for dynamic tuning of reflection bandwidth.

Given the similarities in the formulation and composition of the materials we hypothesize that the electromechanical distortion of the PSCLCs examined here is causing the pitch to expand resulting in a red-shift in the reflection wavelength.
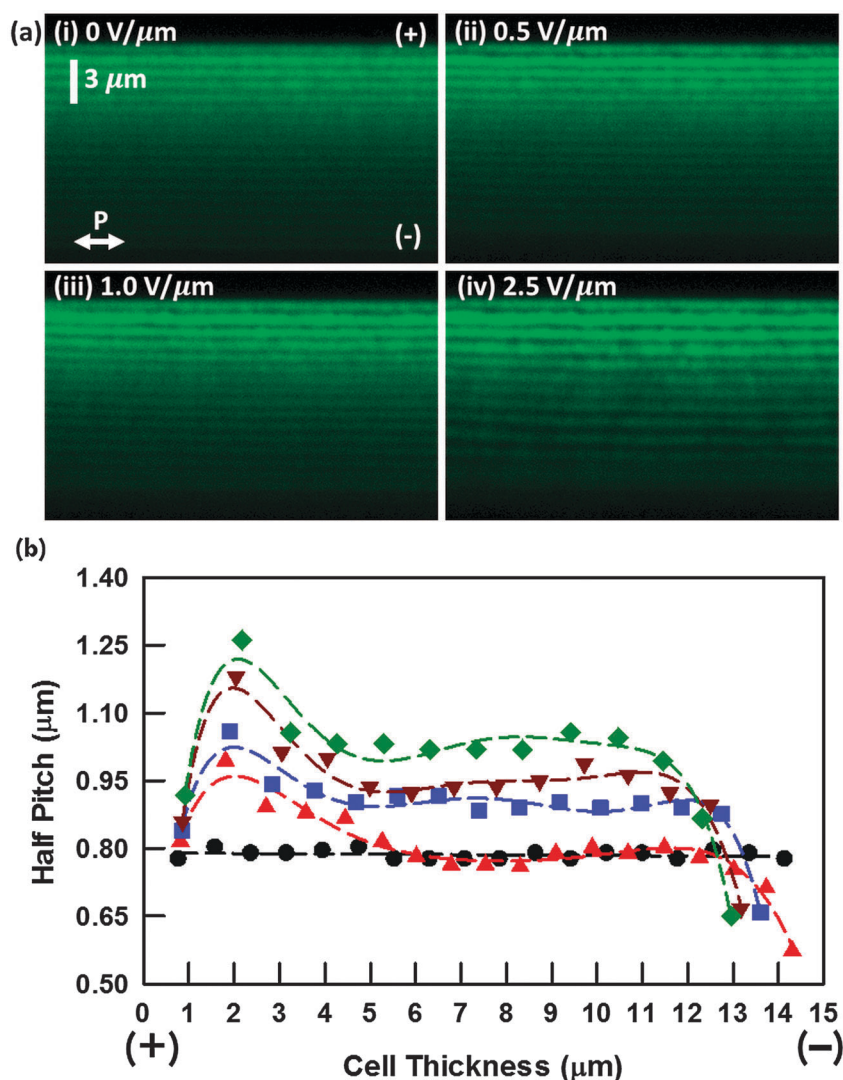

Fig. 4 (a) The 3PEF-PM cross-sectional images of a PSCLC (reflection notch at 2.45 µm) at different DC voltages (i) 0 V µm^{-1}, (ii) 0.5 V µm^{-1}, (iii) 1 V µm^{-1}, and (iv) 2.5 V µm^{-1}. The linear polarization of the 3PEF-PM excitation light is shown using a white arrow marked by "P" and the polarity of DC voltage is indicated using the "+/−" signs. (b) Summary of pitch variation with the increasing the DC voltage across the cell at (●) 0 V µm^{-1}, (▲) 0.5 V µm^{-1}, (■) 1 V µm^{-1}, (▼) 2 V µm^{-1}, and (◆) 2.5 V µm^{-1}.

In order to elucidate the influence of the applied DC field on the pitch variation of the PSCLCs examined here we investigated cross-sectional images of the PSCLC samples using the multi-photon excitation fluorescence polarizing microscopy. Before applying DC voltage, uniform half pitches (spaced at approximately 0.8 µm) are observed at 0 V µm^{-1} shown in Fig. 4(a-i). Optical experiments completed on this sample confirm an initial reflection notch of 2450 nm (not shown here). By assuming an average refractive index of 1.55, this reflection wavelength gives an estimated full pitch length of approximately 1.6 µm. As the strength of the applied DC voltage is increased, the pitches close to the electrodes are influenced first, due to high electric potential near the electrodes. At low DC voltage (0.5 V µm^{-1}), pitches near the positive electrode are expanded as compared to the equilibrium value at no fields, whereas the pitches are contracted near the negative electrode. This is evident in Fig. 4(a-ii) as well as in Fig. 4(b) where around 1–2 pitches are expanded and contracted near the positive and the negative electrodes respectively and nearly 5 pitches in the middle of the cell are seemingly uninfluenced by the applied voltage. As the voltage is increased, the pitches in the middle of the cell gap are expanded somewhat uniformly. Based on the continuous nature of the change in reflection wavelength during the application of DC field, we see no evidence of so-called "pitch hopping" (e.g. an increase or decrease in the relative number of pitches that could emerge as a result of propagation of edge dislocations). Thus, we believe that the relative spacing of the 18 half pitches (9 pitches) observed before applying electric field are dynamically affected by the presence and strength of the applied DC voltage. This is evident in the complex distortion of the pitch across the cell gap shown in Fig. 4(b). Evident in Fig. 4(a-iv), at 2.5 V µm^{-1}, 13 half pitches can be counted. However, the reduction in countable pitches may be caused by the axial resolution limit of the technique to pick up pitches near the opposite side of the cell away from the objective lens. Evident in Fig. 4(b), the red-shifted tuning is attributable to an average increase in pitch specifically relating to the middle portion of the cell gap. Concurrent to the red-shift of the reflection notch, a small increase in reflectivity is observed for example in Fig. 1(a). This reflectivity is likely attributable to the continuous distortion of the pitch near the electrode surfaces that yields a broadband reflection. Due to the use of glass and ITO as a conductive layer, the PSCLC examined here with an original reflection wavelength of 2.45 µm would be expected to shift to 3.25 µm upon application of a 2.5 V µm^{-1} field, or a relative change in pitch ($\Delta p/p_0$) of approximately 30%. From Fig. 1(b), a PSCLC with an initial reflection wavelength of 700 nm has a relative change in pitch ($\Delta p/p_0$) of about 25% at 2.5 V µm^{-1}.

Conclusions

Large magnitude tuning of the reflection notch of polymer stabilized cholesteric liquid crystals (PSCLCs) formulated with negative dielectric anisotropy ($-\Delta\varepsilon$) with excellent out-of-band transmission is reported. Applied DC voltages are shown to induce nonuniform distortion of the pitch across the cell gap. The electro-optic response is attributed to electromechanical deformation of the structural chirality of the polymer stabilizing network, which is visualized with nonlinear optical fluorescence polarizing microscopy. The viscoelastic properties of the polymer network dictate the optical response to sustained application of the DC voltage as well as the relaxation behaviour.

Acknowledgements

Notes and references

1 H.-S. Kitzerow and C. Bahr, *Chirality in Liquid Crystals*, Springer-Verlag, New York, 2001.
2 S.-T. Wu and D.-k. Yang, *Reflective Liquid Crystal Displays*, Wiley, West Sussex, UK, 2001.
3 L.-C. Chien and T. Doi, *U. S. Patent*, 7,090,901, 2006.
4 S. S. Choi, S. M. Morris, W. T. S. Huck and H. J. Coles, *Soft Matter*, 2009, **5**, 354–362.
5 R. Bartolino, A. Ruffolo, F. Simoni and N. Scaramuzza, *Il Nuovo Cimento D*, 1982, **1**, 607–614.
6 D.-K. Yang, J. W. Doane, Z. Yaniv and J. Glasser, *Appl. Phys. Lett.*, 1994, **64**, 1905–1907.
7 D.-K. Yang, J. L. West, L.-C. Chien and J. W. Doane, *J. Appl. Phys.*, 1994, **76**, 1331–1333.
8 M. H. Lu, *J. Appl. Phys.*, 1997, **81**, 1063–1066.
9 B. Taheri, J. W. Doane, D. Davis and D. S. John, *SID Int. Symp. Dig. Tech. Pap.*, 1996, **27**, 39–42.
10 J. Anderson, P. Watson, J. Ruth, V. Sergan and P. Bos, *SID Int. Symp. Dig. Tech. Pap.*, 1998, **29**, 806–809.
11 D.-K. Yang, *J. Disp. Technol.*, 2006, **2**, 32–37.
12 C. C. Li, H. Y. Tseng, T. W. Pai, Y.-C. Wu, W.-H. Hsu, H.-C. Jau, C. W. Chen and T.-H. Lin, *Appl. Opt.*, 2014, **53**, E33–E37.
13 C. Y. Huang, K.-Y. Fu, K. Y. Lo and M.-S. Tsai, *Opt. Express*, 2003, **11**, 560–565.
14 F.-C. Lin and W. Lee, *Appl. Phys. Express*, 2011, **4**, 112201.
15 P. Kumar, S.-W. Kang and S. H. Lee, *Opt. Mater. Express*, 2012, **2**, 1121–1134.
16 M. Xu and D.-K. Yang, *Appl. Phys. Lett.*, 1997, **70**, 720–722.
17 V. P. Tondiglia, L. V. Natarajan, C. A. Bailey, M. M. Duning, R. L. Sutherland, D.-K. Yang, A. Voevodin, T. J. White and T. J. Bunning, *J. Appl. Phys.*, 2011, **110**, 053109.
18 V. P. Tondiglia, L. V. Natarajan, C. A. Bailey, M. E. McConney, K. M. Lee, T. J. Bunning, R. Zola, H. Nemati, D.-K. Yang and T. J. White, *Opt. Mater. Express*, 2014, **4**, 1465–1472.
19 K. M. Lee, V. P. Tondiglia, M. E. McConney, L. V. Natarajan, T. J. Bunning and T. J. White, *ACS Photonics*, 2014, **1**, 1033–1041.
20 H. Nemati, S. Liu, R. S. Zola, V. P. Tondiglia, K. M. Lee, T. J. White, T. J. Bunning and D.-K. Yang, *Soft Matter*, 2015, **11**, 1208.
21 D. J. Broer, J. Lub and G. N. Mol, *Nature*, 1995, **378**, 467–469.
22 R. A. M. Hikmet and H. Kemperman, *Nature*, 1998, **392**, 476–479.
23 M. Mitov, *Adv. Mater.*, 2012, **24**, 6260–6276.
24 R. A. M. Hikmet and H. Kemperman, *Liq. Cryst.*, 1999, **26**, 1645–1653.

25 M. E. McConney, V. P. Tondiglia, L. V. Natarajan, K. M. Lee, T. J. White and T. J. Bunning, *Adv. Opt. Mater.*, 2013, **1**, 417–421.

26 H. Yu, B. Tang, J. Li and L. Li, *Opt. Express*, 2005, **13**, 7243–7249.

27 L. Li, J. Li, B. Fan, Y. Jiang and S. M. Faris, *Proc. SPIE*, 1998, **3560**, 33–40.

28 Z. Li, P. Desai, R. B. Akins, G. Ventouris and D. Voloschenko, *Proc. SPIE*, 2002, **4658**, 7–13.

29 H. Xianyu, S. Faris and G. P. Crawford, *Appl. Opt.*, 2004, **43**, 5006–5015.

30 M. J. Escuti, C. C. Bowley, G. P. Crawford and S. Žumer, *Appl. Phys. Lett.*, 1999, **75**, 3264–3266.

31 F. Simoni, G. Cipparrone and R. Bartolino, *Mol. Cryst. Liq. Cryst.*, 1986, **139**, 161–169.

32 N. Scaramuzza, C. Ferrero, V. Carbone and C. Versace, *J. Appl. Phys.*, 1995, **77**, 572.

33 J. Xiang, Y. Li, Q. Li, D. A. Paterson, J. M. D. Storey, C. T. Imrie and O. D. Lavrentovich, *Adv. Mater.*, 2015, **27**, 3014–3018.

34 L. Lu, V. Sergan and P. J. Bos, *Phys. Rev. E: Stat., Nonlinear, Soft Matter Phys.*, 2012, **86**, 051706.

35 W. Lee, C.-T. Wang and C.-H. Lin, *Displays*, 2010, **31**, 160–163.

36 B. Gosse and J. P. Gosse, *J. Appl. Electrochem.*, 1978, **6**, 515–519.

37 C.-H. Wen, S. Gauza and S. T. Wu, *Liq. Cryst.*, 2004, **31**, 1479–1485.

38 P.-T. Lin, S. T. Wu, C.-Y. Chang and C.-S. Hsu, *Mol. Cryst. Liq. Cryst.*, 2004, **411**, 243–253.

39 S. Naemura, Y. Nakazono, K. Nishikawa, A. Sawada, P. Kirsch, M. Bremer and K. Tarumi, *Mater. Res. Soc. Symp. Proc.*, 1998, **508**, 235–240.

40 K. Neyts, S. Vermael, C. Desimpel, G. Stojmenovik, A. R. M. Verschueren, D. K. G. de Boer, D. K. G. de Boer, R. Snijkers, P. Machiels and A. van Brandenburg, *J. Appl. Phys.*, 2003, **94**, 3891–3896.

41 A. Sawada, *J. Appl. Phys.*, 2006, **100**, 074103.

42 J.-H. Son, S. B. Park, W.-C. Zin and J.-K. Song, *Liq. Cryst.*, 2013, **40**, 458–467.

43 T. Lee, R. P. Trivedi and I. I. Smalyukh, *Opt. Lett.*, 2010, **18**, 3447–3449.

44 R. P. Trivedi, T. Lee, K. A. Bertness and I. I. Smalyukh, *Opt. Express*, 2010, **18**, 27658.

This journal is © The Royal Society of Chemistry 2015

J. Mater. Chem. C, 2015, **3**, 8788–8793 | 8793